Chapter 52
Study of the Tip Surface Morphology of Glass Micropipettes and Its Effects on Giga-Seal Formation

Majid Malboubi, Yuchun Gu, and Kyle Jiang

Abstract Reported is a study of applying nanofabrication technology to improve the surface roughness of micro glass pipettes to achieve giga ohm seal resistance in patch clamping processes. The surface roughness of pipette tips was first measured by 3D reconstruction of pipette tips using stereo imaging technique based on high resolution SEM images. Both the SEM images and the reconstructed images show that micro glass pipettes have rough and uneven tips which could be one of the causes of leakage in patch clamping. Then focused ion beam system was used to cut across the very end of the tip, producing a smooth and flat new tip. The average surface area roughness S_a of a milled pipette tip was within a few nanometres. Patch clamping experiments were carried out using the polished pipettes on human umbilical vein endothelial cells (HUVEC), which were well known for their extremely flat shape making them very difficult to patch. The results show that above 3 GΩ seals were achieved in 60% of the experiments, as opposed to 1.5–2.0 GΩ in average with the conventional pipettes. The highest seal resistance achieved with a focused ion beam polished pipette was 9 GΩ, well above the 3 GΩ resistance, the usually best result achieved with a conventional pipette. The research results demonstrate that the surface roughness of a pipette has a significant effect on the giga-seal formation of a patch clamping process.

Keywords Roughness · giga-seal formation · patch clamping · pipette · focused ion beam

M. Malboubi (✉) and K. Jiang
School of Mechanical Engineering, University of Birmingham, Birmingham, B15 2TT, UK
e-mail: mxm726@bham.ac.uk; k.c.jiang@bham.ac.uk

Y. Gu
School of Medicine, University of Birmingham, Birmingham, B15 2TT, UK
e-mail: y.gu@bham.ac.uk

S.-I. Ao and L. Gelman (eds.), *Electronic Engineering and Computing Technology*, Lecture Notes in Electrical Engineering 60, DOI 10.1007/978-90-481-8776-8_52,

52.1 Introduction

Patch clamp technique has been extensively used for cellular ion channels studies. Introduced by [1], the technique is capable of detecting currents flowing in/out of the cell through a single ion channel at highest resolution. Nowadays it has been proven that many different diseases can be caused by the malfunction of ion channels [2]. The activities of various ion channels under different physical and chemical stimulations and the communications of cells can be studied with the aid of patch clamp method and these studies help us to better understand the fundamentals of cells [3]. In patch clamping a glass micropipette is used to isolate a patch of membrane from external solution to record the currents flowing into the patch. To achieve this small glass capillaries are heated and pulled to fabricate glass micropipettes with a tip diameter of 1–2 μm. The micropipettes are then backfilled with a conductive solution and pressed against the surface of a cell. To improve the sealing condition a gentle suction is applied to the backend of the pipette. As it is shown in Fig. 52.1 there are two electrodes in patch clamp set-up: a recording electrode inside the pipette and a reference electrode in the bath solution. In order to be able to detect single ion channel currents which are in the order of few Pico Amperes, there should be a high resistance seal between the glass and the patch of membrane. The high resistance seal reduces the leakage current between the two electrodes, completes the electrical isolation of the membrane patch and reduces the current noise of the recording [4]. Since the electrical resistance of the seal is in the order of giga-ohms, it is called giga-seal.

The physical and chemical mechanisms behind the giga-seal formation are not fully understood yet, which could probably be a result of high number of different factors important for giga seal formation, such as: the cleanliness of the pipette and cell surface [5, 6], surface roughness of the tip [7–9], geometry of the tip [3, 10], hydrophilicity of the patch site [11, 12], material type [11, 13, 14], glass type of pipette [15, 16], tip size [3], presence of positive ions in the solution [17], gentle approaching of the pipette to the cell membrane [6], vibration of the pipette [4], skill and patience of the operator, etc.

This research work is designed to improve the sealing resistance in patch clamping and to acquire giga-seals more frequently. In this work, the effect of the surface roughness of glass micro pipettes on seal formation was examined. The tip of

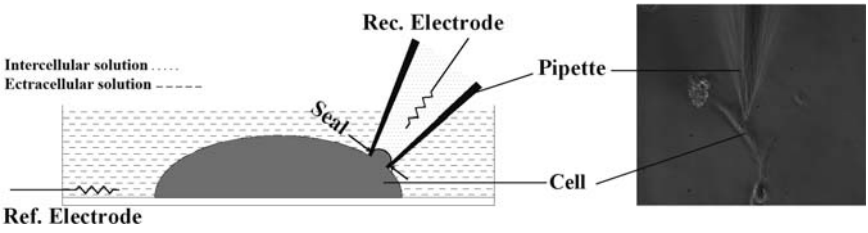

Fig. 52.1 The schematic of the patch clamping method

pipettes were imaged and reconstructed. The surface roughness was measured. The pipette tips were then milled using a focused ion beam (FIB) system resulting in a highly smooth surface. Extensive patch clamp experiments were carried out to investigate the effect of the roughness on seal formation. We call this method "FIB polishing" in comparison with the "fire polishing method". Compared with fire polishing [18,19] the pipettes polished using FIB have much smoother tip surfaces. The nanomachined pipettes were used in patch clamp recording experiments and much improved gigaseal formation has been achieved.

52.2 3D Reconstruction of Micropipette Tip

The glass micro pipettes used in the experiments were made of borosilicate glass pipes with outer diameter of 1.5 mm and inner diameter of 0.86 mm (BF150-86-10 Sutter Instrument). They were heated and pulled with flaming/brown micro pipette puller machine (Sutter Instrument Model P-97). The machine was set to produce pipettes with approximately 1.5 μm in tip diameter. The 3D reconstruction of the pipette tip was based on high resolution scanning electron microscope (SEM) images. Stereoscopic techniques have been widely used to determine the three dimensional structure of an object in which the same area of the object is scanned from different angles by tilting the object with respect to the fixed optic axis [20]. In this technique measurements are made under two different perspectives. Surface features in different heights have different lateral displacements and depth can be calculated by measuring the parallax movement of features from their location in the first image, to the new location in the second image [21]. 3D points are computed from 2D matched points in two SEM images taken from two angles between 5° and 10° away from the norm. Figure 52.2 shows the configuration of SEM, tilting angle (α) and the projected coordination P1(X1, Y), P2(X2, Y).

The third dimension can be found from Eq. (52.1) which can be derived based on the geometry of the projection.

$$Z = \frac{x_2 - x_1 + x_2(1 - \cos\alpha)}{\sin\alpha} \tag{52.1}$$

This process is used for every point of the object to find the shape of the structure [22]. 3D surface profile of the pipette was obtained by analyzing three SEM images using a commercial software package Mex (Alicona) [23]. Figure 52.3 shows the configuration of the FIB polishing and SEM imaging used in the experiments. Also, Fig. 52.4a–c show the SEM images taken from the left, middle and right of the pipette. The tilting angle between (a–b) and (b–c) of the images is 9°. Figure 52.5 shows the 3D reconstructed surface of the pipette tip. It was found that the pipette tip was not only rough, but also wavy or inclined in its form. The surface parameters computed by considering both the roughness and shape of the tip are given in Table 52.1.

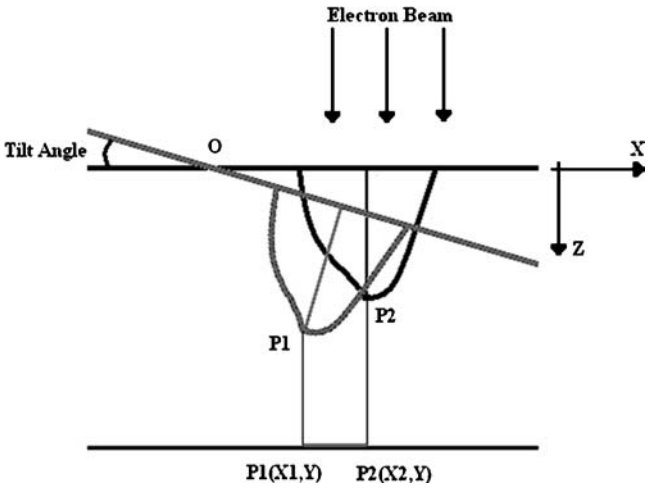

Fig. 52.2 A pair of images of a single object for reconstruction of the object. P1 is the new position of P2 after a tilt of the stage about O

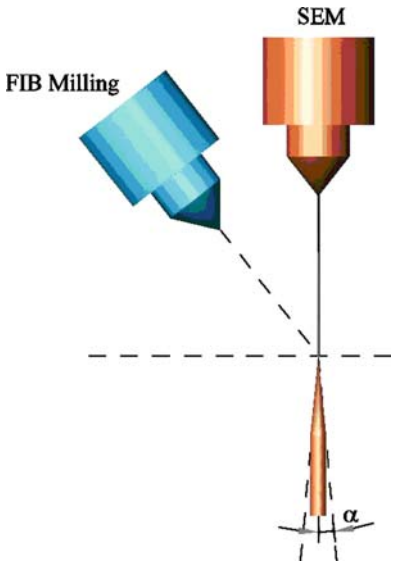

Fig. 52.3 Schematic of the configuration of SEM and the tilting angle (α)

Figure 52.6 shows the shape of the tip along different profiles across the thickness of the pipette. The large variation of the surface morphology shown in Fig. 52.6 increases the chance of ion escape and compromises the formation of high resistance seals. Profile parameters of the profiles are given in Table 52.2.

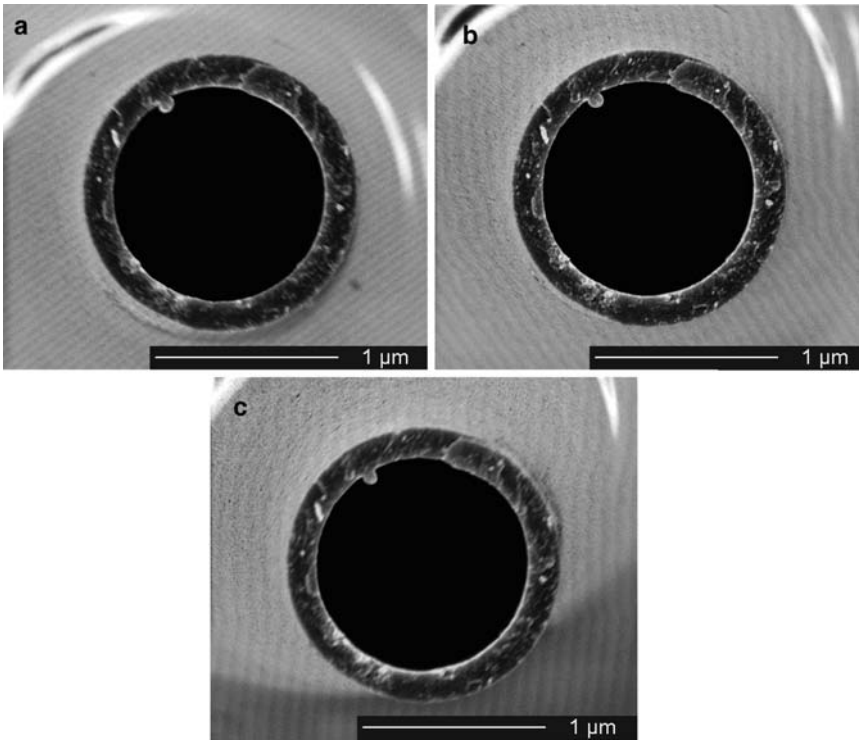

Fig. 52.4 Stereo images of the pipette tip for 3D reconstruction: (**a**) left, (**b**) middle and (**c**) right

Fig. 52.5 A 3D reconstructed surface of the pipette tip shown at different viewing angles; top view (*right*), the exploded view of the area showed by dash-line (*middle*), view with an angle (*right*)

52.3 Focused Ion Beam Polishing

The uneven surface of the pipette tip was corrected by cutting the top of the pipette across using FEI dual beam focused ion beam system. Because of the conic shape of the pipette, cutting the tip changes the tip size which is an important factor in

Table 52.1 Surface parameters of the pipette tip

Name	Value	Description
Sa	27 nm	Average height of selected area
Sq	34 nm	Root-mean-square height of selected area
Sp	104 nm	Maximum peak of selected area
Sv	150 nm	Maximum valley depth of selected area
Sz	255 nm	Maximum height of selected area
Ssk	−0.225	Skewness of selected area
Sku	3.26	Kurtosis of selected area
Sdq	0.877	Root mean square gradient
Sdr	34.98%	Developed interfacial area ratio

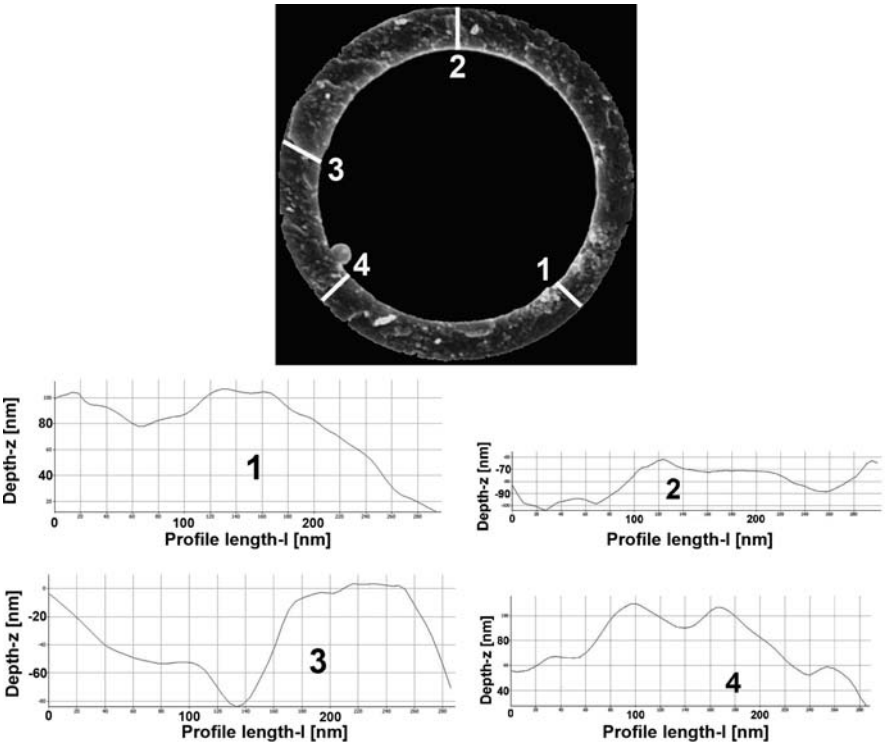

Fig. 52.6 Four different profiles of the tip surface across the thickness are shown. The large variation of surface morphology compromises the formation of a high resistance seal

patch clamping as it determines the pipette resistance. It is also well known that a giga-seal is not likely to be achieved with big tip sizes. So care was taken not to cut more than 1 μm from the top. Since the roughness of the tip of the pipette was in nanometres cutting 1 μm from the top should be sufficient to remove all rough edges

Table 52.2 Profile parameters of four different profiles

Profile	No. 1	No. 2	No. 3	No. 4	Description
Pa	16 nm	8 nm	22 nm	18 nm	Average height of profile
Pq	18 nm	9 nm	25 nm	20 nm	Root-mean-square height of profile
Pt	61 nm	36 nm	95 nm	71 nm	Maximum peak to valley height of primary profile
Pz	21 nm	21 nm	46 nm	31 nm	Mean peak to valley height of primary profile
Pp	30 nm	20 nm	43 nm	30 nm	Maximum peak height of primary profile
Pv	31 nm	16 nm	52 nm	40 nm	Maximum valley height of primary profile
Pc	0 nm	34 nm	79 nm	0 m	Mean height of profile irregularities of primary profile
Psm	0 nm	211 nm	221 nm	0 m	Mean spacing of profile irregularities of primary profile
Psk	0.1269	0.1976	−0.3735	−0.0375	Skewness of primary profile
Pku	1.7548	1.9034	2.0228	1.6307	Kurtosis of primary profile
Pdq	0.5648	0.4698	1.0879	0.7267	Root-mean-square slope of primary profile

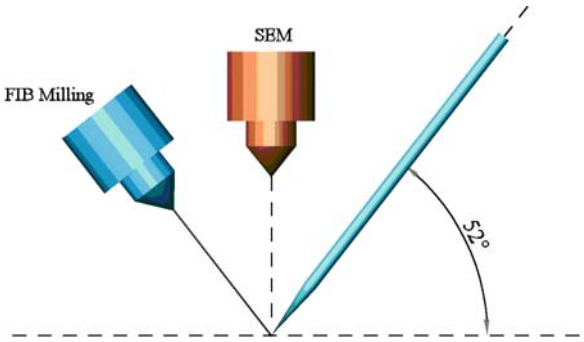

Fig. 52.7 The configuration of glass micro pipette milling in the SEM/FIB chamber. The stage was tilted by 52° so that the ion beam was perpendicular to the pipettes

without increasing the tip size significantly. In the FIB milling process, the pipettes tips were cut using Ga+ ions with 50 pA current for 100 s and dwell time of 1 μs (Fig. 52.7). The pipette before and after milling is shown in Fig. 52.8. The image of the milled pipette, shown in Fig. 52.8 (right), has a resolution of 4.5 nm. No feature could be identified on the milled surface for producing roughness parameters at this magnification. Therefore, the average surface area roughness (Sa) of the milled pipette tip should be less than 4.5 nm.

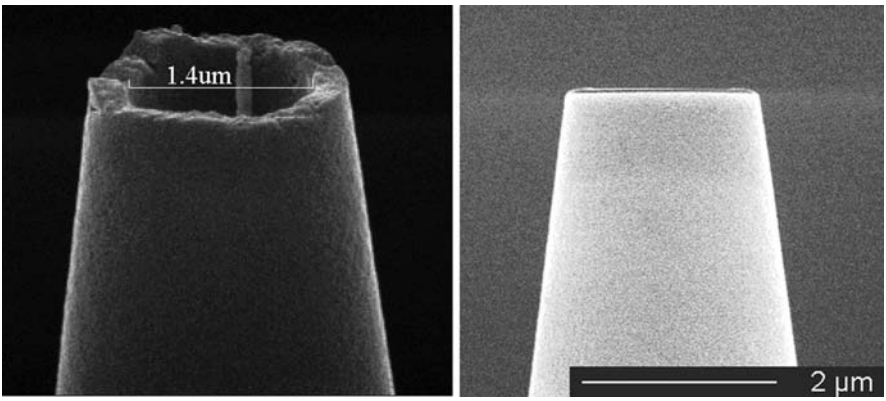

Fig. 52.8 A micro glass pipette before milling (*left*), the pipette after the milling (*right*). No surface roughness could be identified after milling, so the surface roughness should be smaller than the resolution of the SEM image, which is 4.5 nm

52.4 Patch Clamping Experiments

Human umbilical vein endothelial cells (HUVECs) were utilized to investigate the performance of the FIB polished micro pipettes in achieving giga-ohm seals. HUVECs were cultured in EBM medium (Lonza Co., CC-3121) on cover slips 2–3 days before the experiment and incubation was done at 37 °C. At the time of experiments, the confluence of the cells is over 80% and all the cells were firmly attached to the bottom of the cover slips. HUVECs are well known for their extremely flat shape; thus, it is one of the most difficult cell types for patch clamping. During experiments, individual cover slip was directly taken out from incubator and sited in the recording chamber.

Experimental equipment setup consisted of Axon 1D amplifier, Flaming/Brown micro pipette puller (Sutter Instrument Model P-97) and glass micro pipettes (BF150-86-10 Sutter Instrument). The opening of the pipette tip is about 1.4 μm in diameter. The backfill solution contained (in mM): kcl 40, K-gluconate 96, K2ATP 4, GTP 2, HEPE 10, pH 7.2, and the bath solution contained (in mM): NaCl 110, KCl 5, MgCl2 1, CaCl2 1, HEPEs 5, HEPE-Na 5 (mM), pH 7.2.

A 10 mV pulse was constantly applied on the recording electrode from the time that pipette tip was just immersed in the bath solution till it touched the cell membrane. A negative pressure was immediately applied to the pipette and then the voltage pulse was raised to 60 mV to monitor the seal resistance precisely.

To investigate the effect of the roughness of pipette tips, experiments were carried out with polished and conventional pipettes under the same conditions and the results were compared. When there was no contact between recording pipette and cell membrane, the total resistance ranged from 6.0 to 6.5 MΩ. With the FIB polished pipettes, above 3 GΩ seals were achieved in 60% of the experiments ($n = 20$) and the highest seal resistance reached 9 GΩ. In comparison, the seal resistance

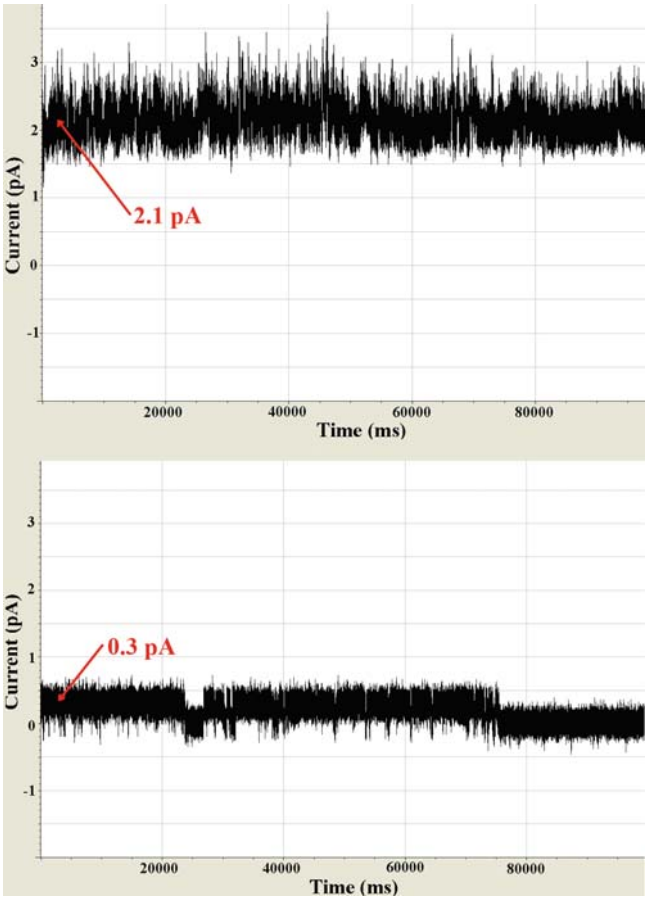

Fig. 52.9 Single channel recording from HUVECs. Conventional pipettes (*top*). FIB polished pipettes (*bottom*)

achieved using the conventional pipettes are 1.5–2.0 GΩ in average and the seal resistance could reach 3 GΩ in some excellent cases. The current in the case of polished pipettes is 0.3 pA, significantly smaller than 2.1 pA achieved using conventional pipettes, indicating higher seal resistance in this case. Single-channel currents recorded from conventional and polished pipettes are shown in Fig. 52.9.

The improved patch clamping performance with polished pipettes is obtained from better contact conditions of the smoother tip surface with membrane. This can be understood as that the smoother surface of the pipette tip leaves little concave area to hold water, opposed to the conventional pipettes, as illustrated in Fig. 52.10. This shows that the membrane can not fill the valleys of the rough surface of conventional pipettes perfectly which could be possibly the reason for reports on lower seal resistance with rough surfaces in the literature. Higher seal greatly reduces the chance of current leakage and reduces the current noise of the recording.

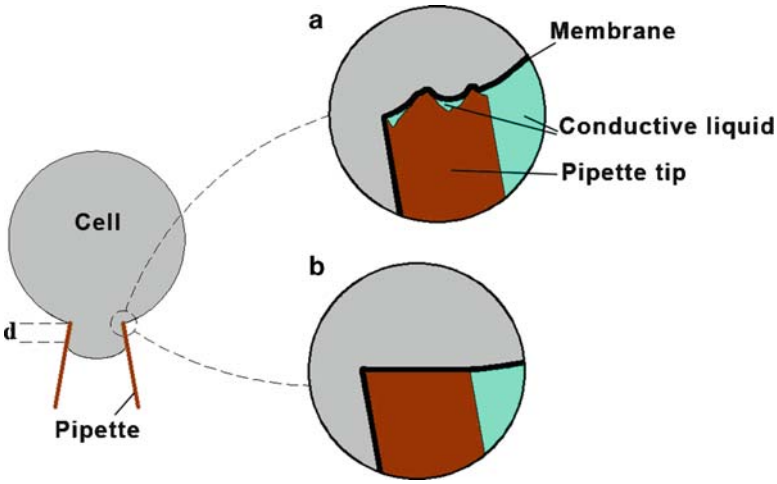

Fig. 52.10 Schematic of pipette-membrane interaction: (**a**) the original pipette tip with a bumpy surface (**b**) the tip is flat

52.5 Discussions and Conclusions

A giga-seal in patch clamping will produce improved signal-to-noise ratio and enables ion channel signal measurement to be more accurate. Currently, the formation of a giga-seal in patch clamping occurs in a sudden and all-or-nothing way. A large number of parameters affect the seal formation, making it hard to understand the physical and chemical mechanisms behind it. In this research, the SEM stereo imaging techniques were used to inspect the surface roughness of micropipettes. The high magnification images revealed the surface nature of the tips to be in contact with cells. Then the contact tips of pipettes were cut across, leaving a very smooth surface at the top of the pipettes. A large number of patch clamping experiments were conducted on HUVECs using the polished pipettes and 60% of the experiments achieved above 3 GΩ seals and the highest seal resistance reached 9 GΩ. The leakage current in single channel recording afterwards was found 0.3 pA, significantly smaller than 2–3 pA usually achieved using conventionally treated pipettes. Smaller current is the consequence of higher seal resistance. The higher seal is obtained from better contact conditions of a smoother tip surface with the cell surface. The results show that nanomachined micro glass pipettes have improved the giga-seal formation in patch clamping.

References

1. Neher, E., Sakmann, B.: Single-channel currents recorded from membrane of denervated frog muscle-fibers. Nature **260**, 799–802 (1976)
2. Dworakowska, B., Dolowy, K.: Ion channel related diseases. Acta Biochim. Polonica **47**(3), 685–703 (2000)

3. Li, S., Lin, L.: A single cell electrophysiological analysis device with embedded electrode. Sens. Actuat. A **134**, 20–26 (2007)
4. Molleman, A.: Patch Clamping: An Introductory Guide to Patch Clamp Electrophysiology. Wiley, England (2003)
5. Hamill, O.P., Marty, A., Neher, E., Sakmann, B., Sigworth, F.J.: Improved patch-clamp techniques for high-resolution current recording from cells and cell-free membrane patches. Euro. J. Physiol. **391**, 85–100 (1981)
6. Stett, A., Burkhardt, C., Weber, U., Stiphout, P., Knott, T.: CYTOCENTERING: A novel technique enabling automated cell-by-cell patch clamping with the CYTOPATCHTM chip. Recep. Channel. **9**, 59–66 (2003)
7. Malboubi, M., Ostadi, H., Wang, S., Gu, Y., Jiang, K.: The effect of pipette tip roughness on giga-seal formation. Proceedings of the World Congress on Engineering (WCE 2009), vol II, London, 1–3 July 2009
8. Matthews, B., Judy, J.W.: Design and fabrication of a micromachined planar patch-clamp substrate with integrated microfluidics. J. Microelectromech. Syst. **15**, 214–222 (2006)
9. Ong, W., Yobas, L., Ong, W.: A missing factor in chip-based patch clamp assay: gigaseal. J. Phys. Conf. Ser. **34**, 187–191 (2006)
10. Lau, A.Y., Hung, P.J., Wu, A.R., Lee, L.P.: Open-access microfluidic patch-clamp array with raised lateral cell trapping sites. Lab Chip **6**, 1510–1515 (2006)
11. Picollet-D'hahan, N., Sauter, F., Ricoul, F., et al.: Multi-Patch: A chip-based ion-channel assay system for drug screening. IEEE ICMENS 2003: International Conference MEMS, NANO & Smart Systems, pp. 251–254, Banff, Alberta, Canada (2003)
12. Ionescu-Zanetti, C., Shaw, R.M., Seo, J., Jan, Y., Jan, L.Y., Lee L.P.: Mammalian electrophysiology on a microfluidic platform. Proceeding of the national academy of science of the united states of America (PNAS) **102**, 9112–9117 (2005)
13. Klemic, K.G., Klemic, J.F., Sigworth, F.J.: An air-molding technique for fabricating PDMS planar patch-clamp electrodes. Euro. J. Physiol. **449**, 564–572 (2005)
14. Zhang, Z.L., Asano, T., Uno, H., et al.: Fabrication of Si-based planar type patch clamp biosensor using silicon on insulator substrate. Thin Solid Films **516**, 2813–2815 (2008)
15. Corey, D.P., Stevens, C.F.: Science and technology of patch-recording electrodes. In: Sakmann, B., Neher, E. (eds.) Single-channel recording, pp. 53–68. Plenum, New York (1983)
16. Levis, R.A., Rae J.L.: Technology of patch-clamp electrodes. In: Walz, W., Boulton, A.A., Baker, G.A. (eds.) Patch-Clamp Analysis Advanced Techniques, pp. 1–35. Humana Press, Totowa, NJ (2002)
17. Priel, A., Gil, Z., Moy, V.T., Magleby, K.L., Silberberg, S.D.: Ionic requirements for membrane-glass adhesion and giga seal formation in patch-clamp recording. Biophys. J. **92**:3893–3900 (2007)
18. Yaul, M., Bhatti, R., Lawrence, S.: Evaluating the process of polishing borosilicate glass capillaries used for fabrication of in-vitro fertilization (iVF) micro-pipettes. Biomed. Microdevice. **10**, 123–128 (2008)
19. Goodman, M., Lockery, S.R.: Pressure polishing: a method for re-shaping patch pipettes during fire polishing. J. Neurosci. Method. **100**, 13–15 (2000)
20. Piazzesi, G.: Photogrammetry with the scanning electron microscope. J. Phys. E: Sci. Instrum **6**, 392–396 (1973)
21. Marinello, F., Bariani, P., Savio, E., Horsewell, A., De, C.L.: Critical factors in SEM 3D stereomicroscopy. Measure. Sci. Technol. **19**, 1–12 (2008)
22. Samak, D., Fischer, A., Rittel, D.: 3D Reconstruction and visualization of microstructure surfaces from 2D images. J. Manufact. Technol. **56**(1), 149–152 (2007)
23. Alicona Imaging GmbH, Austria. http://www.alicona.com. (2010)